

COMPUTATIONAL INVESTIGATION FOR FREE-FLIGHT AERODYNAMICS AND FLIGHT DYNAMICS OF SUBSONIC AND SUPERSONIC PROJECTILES

Qing ZHANG, Zhengyin YE, Shaobo WANG

School of Aeronautics, Northwestern Polytechnical University, Xi'an 710072, P.R.China

Keywords: *Computational Fluid Dynamics, Rigid Body Dynamics, Unsteady Aerodynamics, Spinning Projectile, Trajectory Simulation*

Abstract

In the preliminary design of modern projectiles, numerical simulations could provide the researchers with a greater detail for the flow field, aerodynamic forces and flight trajectories which are very difficult to measure accurately in wind tunnel test or real flight test. Therefore, in this paper, our research team has successfully integrated aerodynamics and flight dynamics into a computational simulation system named GMFlow to solve these coupled problems. And for GMFlow, an advanced time-accurate Navier-Stokes computational technique has been employed to compute the unsteady aerodynamics associated with the free flight of the spinning projectiles at subsonic and supersonic speeds, and an innovatively coupled computational fluid dynamics /rigid body dynamics technique has been used to determine flight trajectories of the projectiles. Unsteady numerical results obtained from the coupled method clearly display the flow field, the aerodynamic forces and moments, and the flight trajectories of the projectiles. Computed positions and orientations of the projectiles have been compared with actual data measured from free flight tests and are found to be generally in decent agreement. Therefore, the actual testing and development costs for projectiles design in the near future could be greatly reduced by the coupled technique which can accurately provide the aerodynamics and flight dynamics for these newly designed configurations.

1 Introduction

There has been a persistent interest in both missiles and projectiles that operate in the high

supersonic to hypersonic range for various missions^[1-5]. With the availability of powerful and fast computing resources, computational methods have attracted great attention during the recent years for unsteady aerodynamic calculations of complex and unconventional configurations^[6-8]. The recent advances made in the high-performance computing and unsteady Computational Fluid Dynamics (CFD) techniques now allow us to compute the total aerodynamic forces and moments needed in the prediction of trajectories directly. The present work is thus focused on the coupling of CFD and rigid body dynamics (RBD) techniques for simultaneous prediction of the unsteady free-flight aerodynamics and the flight trajectory of projectiles^[9-11]. Our goal is to be able to perform time-accurate multidisciplinary-coupled CFD/RBD computations for subsonic or supersonic projectiles based on our newly developed in-house codes GMFlow(Generalized Mesh based Flow solver).

The coupled CFD/RBD procedure allows "virtual fly-out" of projectiles on the supercomputers, and predicts the actual flight paths of a projectile and all the associated unsteady free-flight aerodynamics in an integrated manner. In this coupled procedure, CFD provides the total aerodynamic forces and moments at each time step during the fly-out for a given position/orientation of the projectile. The forces and moments are used as inputs into RBD where the six degree of freedom (6DOF) equations are solved and the new position and orientation of the projectile are determined. CFD is then used to provide solution at the new position and orientation of the projectile in the next time step and the process is repeated. Both CFD and RBD are run in parallel with very

good scalability. Computational time associated with RBD is extremely small compared to CFD and essentially the same scalability is maintained with or without RBD.

Due to the huge computational requirement of the aerospace and related applications, and the rapid development of computer science, CFD has obtained more and more attention^[12~16]. However, the accuracy of CFD is often dependent on the mesh quality, and the high-quality traditional topology mesh is very difficult to be generated for the complex configuration of the time varying space. The arbitrary topology mesh and meshfree method are attractive approaches to improve the mesh quality^[17]. Therefore, GMFlow is developed in our research team for high-resolution spatial discretization of Navier-Stokes (NS) equation based on generalized mesh, and for GMFlow, it unifies the existing mesh topology (structured mesh, unstructured mesh, hybrid mesh, arbitrary topology mesh and meshfree) and thus is convenient to deal with the distorted geometric region, and generate the high-quality mesh. Besides, based on the CFD technique, flight dynamics and aeroelastic analysis modules are also included in our codes. The main work of this paper is to validate the CFD/RBD module of our codes by coupling of aerodynamics and flight dynamics in a time accurate manner to simulate flight trajectories of subsonic and supersonic projectiles.

2 Geometry Description and Computational Technique

Research efforts have been ongoing to perform time-dependent multidisciplinary-coupled CFD/RBD computations for the flight trajectory of complex guided projectile systems. The time-accurate unsteady approach relies on Navier–Stokes equations and 6 DOF computations to compute the trajectories of projectiles. A degree of freedom is a displacement quantity, which defines the location and orientation of an object. In three-dimensional space, a rigid object has six degrees of freedom: three translations and three rotations. The 6 DOF code computes linear and angular velocities as well as the orientation of

the projectile, which are used as input to the computational fluid dynamics code. The time-accurate unsteady approach uses the following simple procedures to compute the trajectories of projectiles. The procedure consists of the following steps:

1) A computational fluid dynamics solver repeatedly solves the Navier–Stokes equations to obtain time-dependent projectile flow field solutions at different attitudes.

2) Aerodynamic forces and moments to be used as input in the 6-degree-of-freedom computations are obtained from flow field solutions.

3) The 6 DOF computations are performed based on flight dynamics equations.

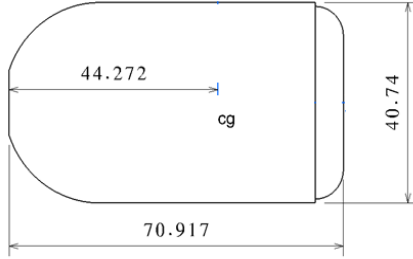
4) Using the new initial conditions from the 6 DOF computations, a true increment in time is taken, and the computational fluid dynamics solver computes a new set of solutions. Both CFD and RBD computations are performed at every time step in a fully coupled manner.

These steps are repeated until the length of the desired trajectory is reached.

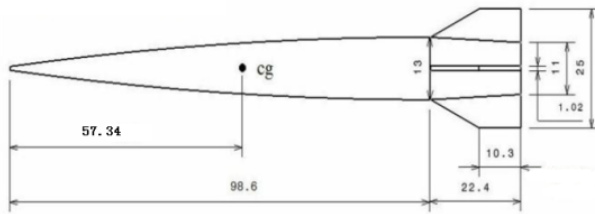
2.1 Geometry Description

Configuration of two projectiles from U.S. Army Research Laboratory is selected as the computational models, since it has detailed experimental data[2~3,7~9]. The first one is a subsonic spinning projectile(see Fig. 1a), and the second one is a supersonic finned projectile(see Fig. 1b). The subsonic projectile is a revolution body comprising an ogive-cylinder configuration with a total length of 70.917mm and a diameter of 40.74mm, and the center of gravity is located at 44.272 mm from the nose of the spinning projectile. The supersonic projectile modeled in this study is an ogive-cylinder-finned configuration. The length of the projectile is 121 mm and the diameter is 13 mm. The ogive nose is 98.6mm long and the afterbody has a 22.4 mm, 2.5 deg boattail. Four fins are located on the back end of the projectile. The fins have a thickness of 1.02 mm, a sweep angle of approximately 30 deg, a 25mm span, a 22.3mm root chord, and a 10.3mm tip chord. The fins have the same constant thickness everywhere, including the leading and trailing

edges. The center of gravity (cg) of the projectile is located 57.34 mm from the nose.



a. Subsonic unfinned projectile



b. Supersonic finned projectile

Fig. 1: Geometric information (all dimensions in mm)

2.2 Numerical Simulations

Time-accurate unsteady numerical computations were performed using Navier-Stokes and coupled 6-DOF methods to predict the flow field and aerodynamic coefficients, and the flight paths of the subsonic and supersonic projectiles. In all cases, full three-dimensional (3D) computations were performed and no symmetry was used. Fully 3D computations are necessary to obtain the desired time-accurate flow solutions.

2.2.1 CFD Computational Technique

The complete set of 3D time-dependent Reynolds-Averaged Navier-Stokes (RANS) equations is solved in a time-accurate manner for simulations of unsteady flow fields associated with both spin-stabilized and finned

projectiles during flight^[6-8]. The 3D time-dependent RANS equations are solved using the finite volume method. The 3D, time-dependent RANS equations are solved using the following finite volume method:

$$\frac{\partial}{\partial t} \int_V W dV + \oint (F - G) \cdot dA = \int_V H dV \quad (1)$$

where \mathbf{W} is the vector of conservative variables, \mathbf{F} and \mathbf{G} are the inviscid and viscous flux vectors, respectively, \mathbf{H} is the vector of source terms, V is the cell volume, and A is the surface area of the cell face. Second-order discretization was used for the flow variables and the turbulent viscosity equations. SA turbulence models were used for the computation of turbulent flows. Dual time-stepping was used to achieve the desired time-accuracy^[8,18], and inner time steps were 500 and 300 while outer time steps were set as $5.0 \times E-05$ s and $1.0 \times E-05$ s for subsonic and supersonic projectiles, respectively.

2.2.2 CFD/RBD Coupling Procedure

Table. 1: Initial conditions for different projectiles

Speed regime	Velocity (m/s)	Euler angles (rad)	Angular velocity (rad/s)
Subsonic	$u = 130.697$	$\varphi = 0.537$	$p = 664.879$
	$v = 15.612$	$\theta = -0.038$	$q = 15.876$
	$w = -2.235$	$\psi = -0.117$	$r = -12.315$
Supersonic	$u = 1030.81$	$\varphi = 2.051$	$p = 2518.39$
	$v = -22.064$	$\theta = -0.088$	$q = 52.802$
	$w = -86.278$	$\psi = 0.023$	$r = -22.233$

To account for rigid body dynamics, the grid point velocities can be set as if the grid is attached to the rigid body with 6 DOF. As shown in Fig. 1, the projectile state vector is comprised of the inertial position components of the projectile mass center (x, y, z), the standard Euler angles (φ, θ, ψ), the body frame components of the projectile mass center velocity (u, v, w), and the body frame components of the projectile angular velocity vector (p, q, r) [7-9]. The entire state vector

consisting of these twelve variables is required in the initial conditions (Table 1) before a virtual free flight can be performed and coupled dynamic solution can be obtained. For the rigid body dynamics, the coupling refers to the interaction between the aerodynamic forces/moments and the dynamic response of the projectile to these forces and moments. In the fully coupled runs, CFD provides the total aerodynamic forces and moments which are used at every time step during the computation of the flight trajectories. The forces and moments are computed every CFD time step and then transferred to a 6-DOF module which computes the body's response to the forces and moments. The response is converted into translational and rotational accelerations that are integrated to obtain translational and rotational velocities and integrated once more to obtain linear position and angular orientation. The 6-DOF rigid body dynamics module uses quaternions to define the angular orientations. However, these are easily translated into Euler angles. From the dynamic response, the grid point locations and grid point velocities are set. Converged solution from this step provides the initial condition for the next step where a completely coupled CFD/RBD computation is performed in time-accurate mode. Here, a complete set of initial conditions includes all translational and rotational velocity components and accounts for initial position and angular orientations. The simulations start from the first station away from the muzzle where the actual data was measured. The first stations are located about 4.549 m and 4.593 m from the muzzle for subsonic and supersonic projectiles respectively.

The centroid translational equation in coordinate system moving with the rigid body is:

$$m\left(\frac{\delta \mathbf{V}}{\delta t} + \boldsymbol{\omega} \times \mathbf{V}\right) = \mathbf{F} \quad (2)$$

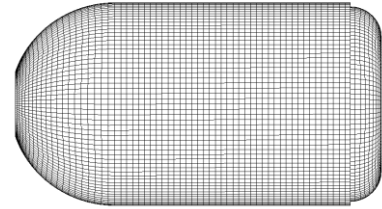
The rotational equation around the mass center under the longitudinal axis is:

$$\frac{\delta \mathbf{h}}{\delta t} + \boldsymbol{\omega} \times \mathbf{h} = \mathbf{M} \quad (3)$$

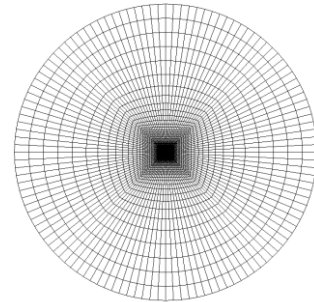
And detailed information could be found in Ref[10,17].

2.3 Computational Grids

In this paper, structured meshes are generated for flow solving, and mesh distributions for the two projectiles are illustrated in Fig.3 and Fig.4, respectively. To accurately capture the flow in the turbulent boundary layer, the spacing near the wall is always much smaller than grids far from the wall. The first grid point spacing from the projectile surface is chosen to achieve a y^+ value of 1.0 based on the flow condition, therefore, it is 2.0×10^{-6} m, 3.0×10^{-7} m for subsonic and supersonic projectile respectively according to its own flow characteristics.



a. Mesh distribution for wall

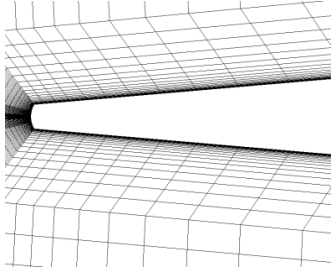


b. Mesh distribution for far field

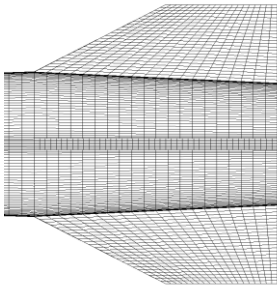
Fig. 2: Structured mesh for subsonic spinning projectile

For both the meshes for the two projectiles, the far field boundary is a column. And for the supersonic mesh, the outflow boundary is three body lengths behind the base of the model, the inflow boundary is just over two body lengths in front of the model, and the circumferential boundary is also just over six body lengths away from the model. The mesh created for the subsonic case was similar in structure to that created for the supersonic case. The far-field boundary was moved further away from the projectile body (Fig. 2) to accommodate the

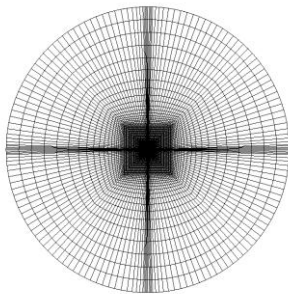
longer recovery distances of flow field features. The new inflow boundary was located just under ten body lengths away, the outflow boundary ten body lengths away, and the circumferential boundary almost twenty body lengths away.



(a) Mesh distribution for nose



(b) Mesh distribution for fins



(c) Mesh distribution for far field

Fig. 3: Structured mesh for supersonic finned projectile

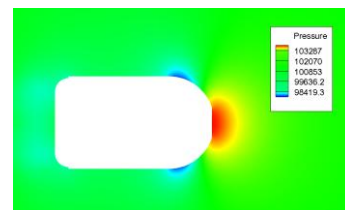
A moving grid technique must be employed to simulate the trajectories of projectiles^[19-21]. A number of strategies have been formulated along the years depending on the complexity of the application. The unsteady aerodynamic solution of the body requires the moving boundary at each time step. The dynamic mesh algorithm moves the computational mesh to conform to the instantaneous position of the moving boundary at each time step. In this study, the moving grid technique can be significantly

simplified when the problem deals with rigid displacements. In such a case, the measurement of the control volumes do not change with time and the fluid motion can be merely simulated through translation and rotation operations without invoking any grid regeneration procedure.

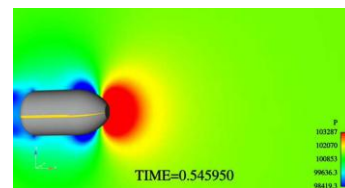
3 Results and Discussions

Time-accurate unsteady numerical computations were performed using Navier-Stokes and coupled 6-DOF methods to predict the flow fields, aerodynamic coefficients, and the flight paths of projectiles at subsonic and supersonic speeds. In all cases, full 3D computations using atmospheric flight conditions were performed and no symmetry was used. Fully 3-D computations are necessary to obtain the desired time-accurate solutions. Typically we begin with a computation performed in “steady state mode” with the grid velocities prescribed to account only for the translational motion component of the complete set of initial conditions to be prescribed, then continue the calculation with rotational motion included till flow solutions converge.

3.1 For Spinning Projectile at Subsonic Speed



(a) From GMFlow



(b) From Ref[2]

Fig. 4: Comparison of pressure contour at $t=0.545950s$

Accurate pressure predictions are critical for trajectory simulation because the aerodynamic forces and moments are integrated from the unsteady pressures. Figure 4 shows the computed pressure contours for the spinning projectile from our own codes GMFlow and Ref[2] at a given location in the trajectory, and it is clearly show that the computed results are generally in a good agreement. Besides, it displays the orientation of the body at that instant in time and the resulting asymmetric flow field in the wake due to the body at angle of attack. The orientation of the projectile of course changes from one instant in time to another as the projectile flies down range. This includes the Euler pitch and yaw angles as well.

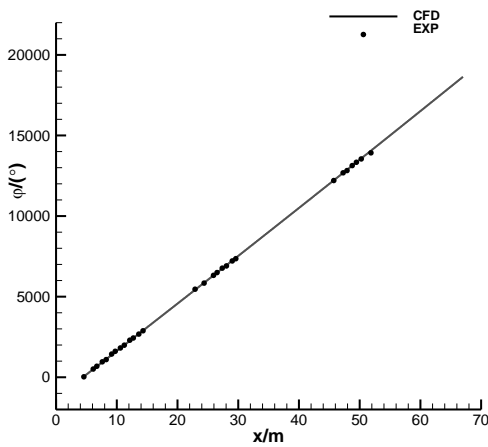


Fig. 5: Comparison of Euler roll angle from CFD and experimental data

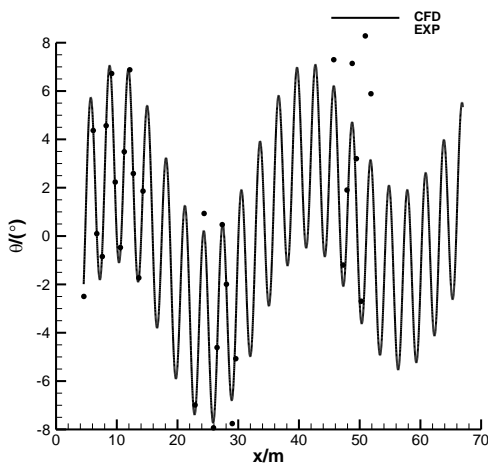


Fig. 6: Comparison of Euler pitch angle from CFD and experimental data

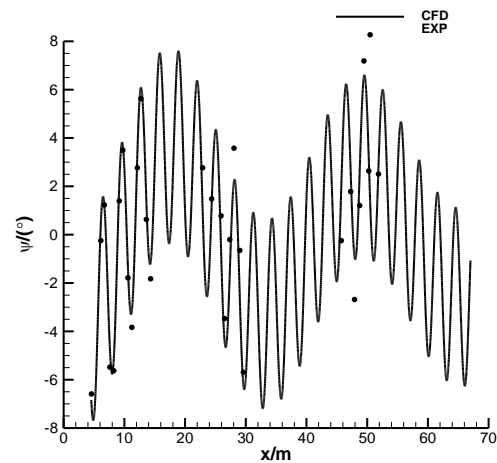


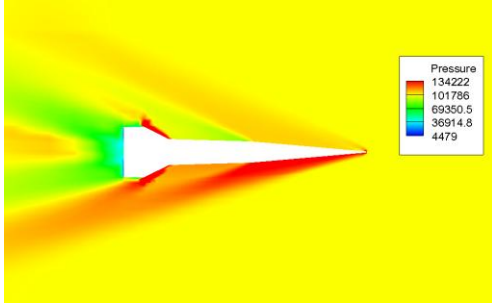
Fig. 7: Comparison of Euler yaw angle from CFD and experimental data

Figures 5~7 show the comparisons of Euler roll, pitch, and yaw angles from computational and actual flight results as a function of x range for spinning projectile at subsonic speed. The computed roll angles are found to increase with increasing x distance results, and both pitch and yaw angles change in a sinusoidal tendency, and from these figures, we can clearly see that computed results are generally found to be in good agreement with the measured data, which demonstrate the accuracy of GMFlow for subsonic projectile trajectory simulation.

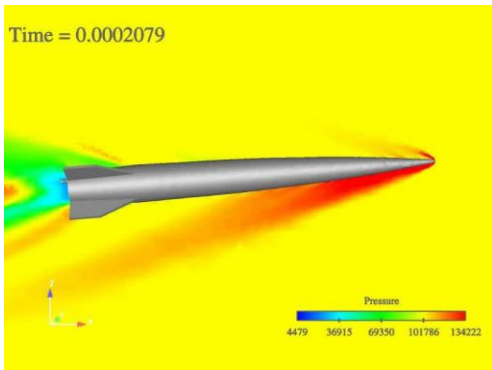
3.2 For Finned Projectile at Supersonic Speed

Figure 8 shows the computed pressure contours for the finned projectile from our own codes GMFlow and Ref[7] at a given location, and it is clearly show that the computed results are generally in a good agreement. In the flight process, the freestream and the longitudinal axis of the projectile are not parallel to each other, so the shock wave at the front of the projectile and the flow pressure are asymmetric at upper side and lower side. The high rotational velocity also makes the pressure distribution on the two surfaces of a fin different. If the outward normal direction of the fin surface is as same as the rotation direction, the pressure on this side is higher than the other side. The asymmetric pressure on two sides of fins forms a moment opposite to the rotation orientation, which results in the decrease of the

rotation velocity of the projectile in the flight process. It clearly shows the orientation of the body at that instant in time and the resulting asymmetric flowfield due to the body at angle of attack in Fig.8. Of course, the orientation of the projectile changes from one instant in time to another as the projectile flies down range.



(a) From GMFlow



(b) From Ref[2]

Fig. 8: Comparison of pressure contour at $t=0.0002079s$

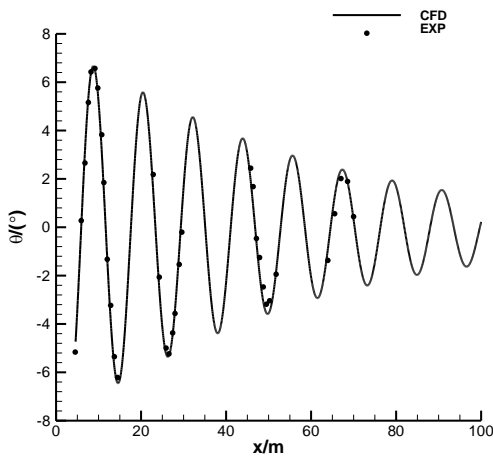


Fig. 9: Comparison of Euler pitch angle from CFD and experimental data

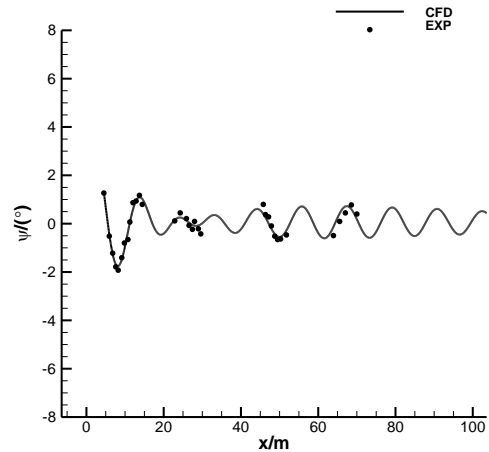


Fig. 10: Comparison of Euler yaw angle from CFD and experimental data

Figures 9~10 show the comparisons of Euler pitch, and yaw angles from computational and actual flight results as a function of x range for finned projectile at supersonic speed. Both the computed pitch and yaw angles change in a sinusoidal tendency, and from these two figures, we can clearly see that computed results are generally found to be in good agreement with the measured data, which demonstrate the accuracy of GMFlow for supersonic projectile trajectory simulation.

4 Concluding Remarks

This paper describes a coupled CFD/RBD computational study undertaken based on GMFlow to simultaneously determine the flight trajectory and the associated unsteady free-flight aerodynamics of projectiles using structured rigid grids at subsonic and supersonic flow speeds. A full three-dimensional unsteady structured Navier-Stokes solver is employed to compute the time-accurate flow fields for the projectile and computed results have been obtained using coupled CFD/RBD virtual free flight simulations. Computed positions and orientations of the two projectiles have been agreed well with experimental results obtained from U.S. Army Research Laboratory.

Technologies developed in this research provided critical information such as the trajectory and attitude, and associated unsteady aerodynamic effects required for design and

control of spinning projectiles in flight. Considering the efforts and cost reduction for smart munitions development by CFD comparing to wind tunnel experiment or real flight test, it is concluded that multidisciplinary coupled CFD and rigid body dynamics predictions based on our newly developed in-house codes GMFlow is an accurate and efficient method for preliminary design of new configurations in the future.

Acknowledgement

This work would not been accomplished successfully without the financial support of National Natural Science Foundation of China under the grant No.11272262. Besides, the authors wish to thank Dr. Lei Yang for his patient discussion and assistance on coupling process between aerodynamics and flight dynamics. The authors also wish to thank Dr. Fei Liao for his sincere help on solutions and analysis of unsteady flow field around those projectiles in this paper.

References

- [1] DeSpirito J., and Heavey R.K. CFD Computation of Magnus Moment and Roll Damping Moment of a Spinning Projectile. AIAA Atmospheric Flight Mechanics Conference and Exhibit, Providence, Rhode Island, AIAA 2004-4713, pp 1-16, 2004.
- [2] Sahu, J. Time-accurate Computations of Free-Flight Aero-dynamics of a Spinning Projectile with and without Flow control, AIAA Atmospheric Flight Mechanics Conference and Exhibit, Keystone, Colorado, AIAA 2006-6006, pp 1-10, 2006.
- [3] Sahu, J. Computations of Unsteady Aerodynamics of a Spinning Body at Transonic Speeds, 27th AIAA Applied Aerodynamics Conference, San Antonio, Texas, AIAA 2009-3852, pp 1-11, 2009.
- [4] Damljanić D., Mandić, S., and Vuković D. Computational Fluid Dynamics and Wind Tunnel Determination of the Aerodynamic Characteristics of an Axi-Symmetric projectile with a Conical Tail Flare, Scientific Technical Review, Vol.61, No.3-4, pp 49-58, 2011.
- [5] Muthukumaran C.K., Rajesh G., and Kim, H.D. Launch Dynamics of Supersonic Projectiles, Journal of Spacecraft and Rockets, Vol. 50, No. 6, pp1150–1161, 2013.
- [6] Sifton S. I. Navier–Stokes Computations for a Spinning Projectile for Subsonic to Supersonic Speeds, Journal of Spacecraft and Rockets, Vol. 42, No. 2, pp 223–231, 2005.
- [7] Sahu, J. Unsteady Flow Computations of a Finned Body in Supersonic Flight, ARL-TR-3603; U.S. Army Research Laboratory: Aberdeen Proving Ground, MD, 2005.
- [8] Sahu, J. Time-accurate Numerical Prediction of Free-flight Aerodynamics of a Finned Projectile, Journal of Spacecraft and Rockets, Vol.45, No.5, pp 946-954, 2008.
- [9] Sahu J., Costello M., and Montalvo C. Development and Application of Multidisciplinary Coupled Computational Techniques for Projectile Aerodynamics, Seventh International Conference on Computational Fluid Dynamics, Big Island, Hawaii, pp 1-19, 2012.
- [10] Wang G., Zeng Z., and Suo Q. Trajectory Simulation of a Spinning Projectile Based on Variable Step Size CFD/BD Method, AIAA Atmospheric Flight Mechanics Conference, Kissimmee, Florida, AIAA 2015-0522, pp 1-12, 2015.
- [11] Hua R.H., Zhao C.X., Ye Z.Y., and Jiang, Y.W. Effect of elastic deformation on the trajectory of aerial separation, Aerospace Science and Technology, Vol. 45, No. 9, pp 128–139, 2015.
- [12] Zhang Q., Hua R.H., and Ye Z. Y. Experimental study on a novel method for vertical tail buffet suppression, Journal of Experiments in Fluid Mechanics, Vol. 29, No. 1, pp 37–42, 2015.(in Chinese)
- [13] Zhang Q., and Ye Z. Y. Study on a New Method for Suppression of Vertical Tail Buffeting Using Inflatable Bumps, Engineering Mechanics, Vol. 31, No. 12, pp 234–240, 2014. (in Chinese)
- [14] Zhang Q., and Ye Z.Y. Novel Method Based on Inflatable Bump for Vertical Tail Buffeting Suppression, Journal of Aircraft, Vol. 52, No. 1, pp 367–371, 2015.
- [15] Zhang Q., Hua R.H., and Ye Z. Y. Experimental and computational investigation of novel vertical tail buffet suppression method for high sweep delta wing, SCIENCE CHINA Technological Sciences, Vol. 58, No. 1, pp 147–157, 2015.
- [16] Liao F., Ye Z. Y., and Zhang, L.X. Extending geometric conservation law to cell-centered finite difference methods on stationary grids, Journal of Computational Physics, Vol. 284, pp 419–433, 2015.
- [17] Jiang., Y.W. Numerical Solution of Navier-Stokes equations on Generalized Mesh and Its Applications, Ph.D dissertation, Northwestern Polytechnical University, 2012.
- [18] Zhang L. P., and Wang Z. J. A Block LU-SGS Implicit Dual Time-Stepping Algorithm for Hybrid

Dynamic Meshes, Computers and Fluids, Vol. 33, No. 7, pp 891–916, 2004.

- [19] Kim H.D., Setoguchi T., and Matsuo S. Numerical Simulations of the Projectile Aerodynamics using a Moving Coordinate Method, Proceedings of the 3rd BSME-ASME International Conference on Thermal Engineering , Dhaka, Bangladesh, pp 1-19, 2006.
- [20] Massey K.C., and Sifton S. I. Combining Experimental Data, CFD, and 6-DOF Simulation to Develop a Guidance Actuator for a Supersonic Projectile, 3rd International Symposium on Integrating CFD and Experiments in Aerodynamics, U.S. Air Force Academy, CO, USA, pp 1-10, 2007.
- [21] Costello M., Gatto S., Sahu J., Using CFD/RBD Results to Generate Aerodynamic Models for Projectile Flight Simulation, AIAA Atmospheric Flight Mechanics Conference, Hilton Head, South Carolina, AIAA 2007-6582, pp 1-22, 2007.

Contact Author Email Address

Qing ZHANG, Ph.D. student, E-mail:
zhangqing2220@mail.nwpu.edu.cn Tel:+86
029-88491374

Zhengyin YE, Professor, E-mail:
yezy@nwpu.edu.cn

Shaobo WANG, graduate, 277462810@qq.com

Copyright Statement

The authors confirm that they, and/or their company or organization, hold copyright on all of the original material included in this paper. The authors also confirm that they have obtained permission, from the copyright holder of any third party material included in this paper, to publish it as part of their paper. The authors confirm that they give permission, or have obtained permission from the copyright holder of this paper, for the publication and distribution of this paper as part of the ICAS proceedings or as individual off-prints from the proceedings.